Selectivity control in the reaction between 2-hydroxyarylaldehydes and 4-hydroxycoumarin. Antioxidant activities and computational studies of the formed products

Kamilia Ould Lamara, Malika Makhloufi-Chebli, Amina Benazzouz-Touami, Souhila Terrachet-Bouaziz, Nejla Hamdi, Artur M.S. Silva, Jean-Bernard Behr

ELSEVIER

Journal of Molecular Structure
journal homepage: www.elsevier.com

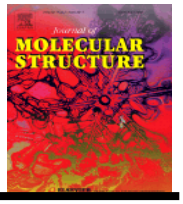

Selectivity control in the reaction between 2-hydroxyarylaldehydes and 4-hydroxycoumarin. Antioxidant activities and computational studies of the formed products

Kamilia Ould Lamara,[a] *Malika Makhloufi-Chebli,*[a]* *Amina Benazzouz-Touami,*[a] *Souhila Terrachet-Bouaziz,*[b,c] *Nejla Hamdi,*[d, e] *Artur M.S. Silva,*[f] *and Jean Bernard Behr*[g]**

[a] *Laboratoire de Physique et Chimie des Matériaux LPCM, Faculté des Sciences, Université Mouloud Mammeri, 15000, Tizi Ouzou, Algeria.*

[b] *Department of Chemistry, Faculty of Sciences, University Mohamed Bouguerra, Boumerdes, Algeria.*

[c] *Laboratoire de Physico-Chimie Théorique et de Chimie Informatique, Faculté de Chimie, USTHB, BP 32 El Alia, 16111 Bab-Ezzouar, Alger, Algeria.*

[d] *Centre de Recherche Nucléaire de Draria (CRND), BP 43, Sebala, Draria, Algeria.*

[e] *Département du Génie de l'environnement, Ecole Nationale Polytechnique, 10 Avenue des Frères Ouadek, Hassen Badi, BP 182, 16200 El Harrach, Algiers, Algeria.*

[f] *QOPNA & LAQV-REQUIMTE, Department of Chemistry, University of Aveiro, 3810-193 Aveiro, Portugal.*

[g] Université de Reims Champagne Ardenne, CNRS, ICMR UMR 7312, 51097 Reims, France.

ARTICLE INFO

Article history:
Received
Received in revised form
Accepted
Aqavailable online

Keywords:
Coumarin
Antioxidant activity
Molecular docking
Molecular dynamics
Cancer
P38 MAPK protein

ABSTRACT

A series of *6H,7H*-7-(4-Hydroxy-3-coumarinyl)[1]benzopyrano[4,3-b][1]benzopyran-6-ones **4a-g** and 3-(2-hydroxybenzoyl)-2*H*-chromen-2-ones **5a-g** derivatives were synthesized by reaction of 4-hydroxycoumarin with 2-hydroxyarylaldehydes **2a-f** or 2-hydroxynaphtaldehyde **2g** using different solvents and acid/base catalysts. The approach relies on a regioselective cascade reaction involving one/two molar equiv of the 4-hydroxy coumarin iteratively acting as active methylene substrate in a Knoevenagel condensation and in a Michael addition. The structures of all compounds were established by IR, mass spectrometry, ^{1}H-NMR and ^{13}C-NMR. Antioxidant activity of the synthesized compounds were determined using the DPPH scavenging assay, best results being obtained with **5b** (IC_{50} = 236 µg/mL). Computational studies showed that the compounds bind in the ATP-binding site of p38 MAPK, in a same manner than known polyaromatic potent inhibitors. The synthesized compounds might be considered further for cancer therapy.

1. Introduction*

Due to its versatile properties, the coumarinyl substructure is a priviledged scaffold in the design of organic compounds. Notwithstanding its particular physico-chemical behavior as a powerful fluorogenic conjugate, the 2-chromenone moiety is also found in natural products and highly bioactive compounds. Indeed, coumarin-derived drugs exhibit broad biological activity with, for example, antioxidant, anticoagulant, antifungal, anthelmintic, or hypnotic properties [1–10]. Anticancer properties of chromenones have also been reported. Recently, Batran and collaborators demonstrated that coumarin derivatives act as potent anti-breast and anti-cervical cancer agents [11]. In this domain, one of the possible targets of coumarin-derived compounds is the p38 mitogen-activated protein kinase (p38 MAPK) that regulates a large number of cellular pathways and plays an important role in cell survival and apoptosis. This was confirmed by other studies reporting the intervention of p38 MAPK inhibitors on cancer cell death [12]. Thus, coumarin appears as an attractive chemical scaffold for the development of new anticancer agents, which would target p38 MAP-kinase as the biological receptor. Numerous methods have been devised for the functionalization of

*Corresponding author. Laboratoire de Pysique et Chimie des Matériaux LPCM, Faculté des Sciences, Université Mouloud Mammeri, 15000, Tizi-Ouzou, Algéria.
e-mail adresses : makhloufi_malika@yahoo.fr (MM),
jb.behr@univ-reims.fr (JBB)

coumarin, among which the reaction with 2-very few number of investigations have been carried out on the reactivity of 4-hydroxycoumarin **1** vis-a-vis ortho-hydroxy arylaldehydes **2**, the outome of the reaction seemed particularly dependent on the reaction conditions. In their pioneering work in 1943 W. R. Sullivan and coworkers [13] reported the condensation of 4-hydroxycoumarin with o-hydroxybenzaldehyde in refluxing ethanol affording two products, to which they attributed the structures of the 1:1 adduct **3a** and of the 2:1 adduct **4** as shown on scheme 1. However, the chemical structure of **3a** was unambiguously corrected in 1984 to its regioisomer **5**. Formation of **5** can be explained by a subsequent intramolecular translactonization from unstable intermediate **3a**, which occurs spontaneously in absence of any catalyst. This translactonization has already been revisited and described in our laboratory by M. Makhloufi and all [14]. The authors used apolar medium (toluene) in the presence of triethylamine (NEt_3) or KF-Al_2O_3 (10%) to initiate the transformation.

Years later, Xiang-Shan Wang and all [15] experienced the condensation of o-hydroxyarylaldehydes with an excess of 4-hydroxycoumarin (2:1) in ethanol, using KF-Al_2O_3 as a catalyst. Surprisingly, in these conditions the 2:1 adduct **6** was obtained almost exclusively, with no traces of the expected 2:1 adduct **4**. Whereas **4** results from intramolecular addition/elimination between OH from the salicylaldehyde moiety and coumarinyl C=O, an identical reaction between both the coumarinyl moieties accounts for the formation of **6**. Even more astounding was the result obtained in an aqueous medium when triethylbenzylammonium chloride hydrate (TEBAC-H_2O) was used as catalyst. In this case the 1:1 adduct **5**, the *E*-stereoisomer of **3a**, was obtained as a stable product in good yields (84%). According to these results, the reaction of o-hydroxyaldehydes with 4-hydroxycoumarin appears as a highly versatile option to prepare new series of coumarin-based conjugates. The variety of products which might be accessed under various conditions justifies the idea of revisiting this reaction to probe chemico- and regio-selectivity. In this study, the reaction of 4-hydroxycoumarin with a series of o-hydroxyarylaldehydes was performed under various solvent, catalyst or activation conditions to control the formation of the two possible poly-heterocyclic products. We also report the evaluation of the antiradical activity of the synthesized compounds using the DPPH scavenging assay. In addition, molecular docking and molecular dynamics studies were performed for compounds **4a** and **5a** in order to evaluate their potential as p38 MAPK inhibitors.

2. Experimental section

2.1. General

Melting points were determined on a Stuart scientific SPM3 apparatus fitted with a microscope and are uncorrected. ^1H and ^{13}C NMR spectra were recorded in DMSO-d6 solutions on Bruker Avance 300 (300.13 MHz for ^1H and 75.47 MHz for ^{13}C) spectrometer. Chemical shifts are reported in parts per million (δ, ppm) using TMS as internal reference and coupling constants (*J*) are given in hertz (Hz). Mass spectra are obtained with ESI. Positive-ion ESI mass spectra were acquired using a Q-TOF 2 instrument [diluting 1 mL of the sample chloroform solution (10^{-5} M) in 200 µL of 0.1% trifluoroacetic hydroxybenzaldehydes appears of broad versatility. Although acid/methanol solution. Nitrogen was used as nebulizer gas and argon as collision gas. The needle voltage was set at 3000 V, with the ion source at 80 °C and desolvation temperature at 150 °C. Cone voltage was 35 V]. The elemental microanalysis (C, H, N) was carried out by the Truspec 630-200-200 Elementary Analysis-Equipment.

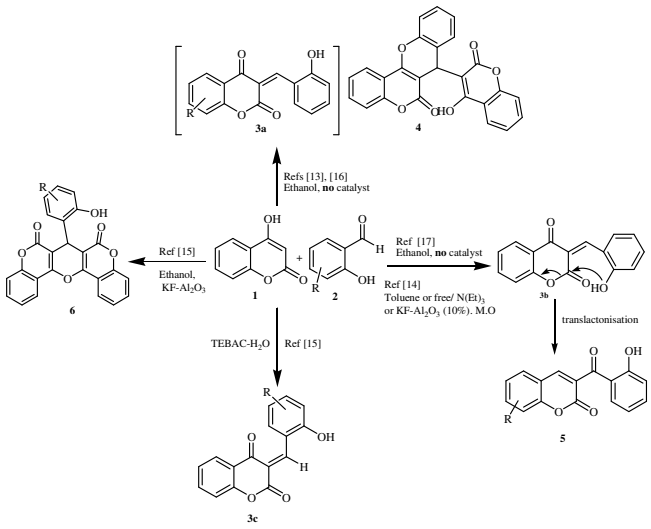

Scheme 1. Selectivity of the reaction of o-hydroxyaldehydes with the 4-hydroxycoumarin.

2.2. Procedure for the synthesis of 5-iodosalicyaldehyde

To a dry 500 ml round bottom flask, 14 ml (0.134 mol) of salycilaldehyde and 300 ml of methanol were added and stirred until complete dissolution. While maintaining magnetic stirring 20.07 g (0.134 mol) of sodium iodide (NaI) were added. After complete dissolution of the NaI the beaker was placed on an ice/water bath. Carefully **1eq** of chloramine T was added to the reaction mixture, magnetic stirring was maintained for 60 minutes keeping the temperature at 0°C. After removal of the ice bath, 100 ml of a 10% (w/w) aqueous solution of sodium thiosulfate was added while stirring for further 5 minutes. Under magnetic stirring, acidification of the reaction mixture was carried out with an HCl solution (2M, about 10 ml) until a yellow precipitate formed (PH 3-4). The solid obtained was filtered, washed with cold distilled water, dried and then recrystallized from dilute ethanol (v/v) to obtain the iodosalicylaldehyde as light yellow crystals. Yield 60 %, mp 98 °C, IR (KBr): 3220 (broad, OH), 2974 (CH aliphatic), 1668 (C=O), 1604 (C=C aromatic), 557 (C-I). ^1H-NMR (DMSO-D_6): δ 10.93 (*s*, 1H, OH), 10.16 (*s*, 1H, CHO), 7.87 (*d*, *J*=2.5, 1H, HAr), 7.77 (dd, *J*=9.0, *J*=2.5, 1H, HAr), 6.85 (d, *J*=9.0, 1H, ArH).

2.3. General procedure for the synthesis of 6H,7H-7-(4-Hydroxy-3-coumarinyl)[1]benzopyrano[4,3-b][1]benzopyran-6-ones (4a-g) and 3-(2-hydroxybenzoyl)-2H-chromen-2-ones (5a-g)

A dry flask was charged with 4-hydroxy-2*H*-chromen-2-one **1** [(1 equiv, 5 mmol) or (2 equiv, 0.1 mmol)], the appropriate salicylaldehyde derivative (and 2-

hydroxynaphtaldehyde) **2a-g** (1 equiv, 5 mmol) and in free or in the presence of an amount of catalyst (see Table 1 and Table 2), in solvent (20 mL). The mixture was stirred and refluxed. The obtained solid was filtered off and washed with hot methanol and was identified as compound **4a-g** (solid not soluble in hot methanol obtained by filtration before cooling) and **5a-g** (obtained from the filtrate after cooling).

_6H,7H_-7-(4-Hydroxy-3-coumarinyl)[1]benzopyrano[4,3-b][1]benzopyran-6-one (4a)

White powder, mp 241-243° C; IR υ (cm^{-1}): 2972, 1699, 1645, 1610, 1567, 1488, 1455, 1390, 1276, 1242, 1221, 1106, 1044, 979, 905, 866, 757 cm^{-1}, ^{1}H NMR (DMSO-D_6): δ 5.75 (s, 1H, H*), 7.15–7.68 (m, 11H, ArH), 8.09–8.12 (d, *J*=8.1 Hz , 1H, ArH), 12.20 (br s, OH-pyr); RMN ^{13}C (DMSO-D_6,): δ 28.7 (C*), 100.6, 106.1, 113.9, 116.1, 116.2, 116.5, 122.2, 122.6, 123.9, 124.5, 125.3, 128.3, 128.6, 132.2, 132.5, 149.2, 151.7, 152.2, 156.3 160.4. ms (ESI): m/z (% relative intensity): 433.2 (100 %) ($M+Na^+$). Elemental analysis: Calcd. For $C_{25}H_{14}O_6$: C 73.17; H 3.44; Found: C 73.20; H 3.50.

10-Hydoxy-_6H,7H_-7-(4-Hydroxy-3-coumarinyl)[1]benzopyrano[4,3-b][1]benzopyran-6-one (4b)

White powder, mp 265-267 °C; ^{1}H NMR (DMSO-D_6): δ 5.71 (s, 1H, CH), 6.61 (d, J=6.63Hz , 1H, ArH) 6.82 (d, *J= 6.8 Hz* , 1H, ArH), 7.32-7.50 (m, 5H, ArH), 7.52 (t, 1H, ArH), 7.76 (t, 1H, ArH), 8.31 (d, *J*=8.3 Hz, 1H, ArH), 9.85 (br s, OH-Ar), 12.20 (br s, OH-pyr.); RMN ^{13}C (DMSO-D_6): δ 28.7 (C*), 107.3, 114.0, 115.5, 116.1,116.2,116.3, 118.3,123.2, 123.9, 124.4, 125.2, 132.2, 132.4, 145.1, 151.9, 152.1, 160.5. ms (ESI): m/z (% relative intensity): 449.2 (100%) ($M+Na^+$). Elemental analysis: Calcd. For: $C_{25}H_{14}O_7$: C 70.42; H 3.31; Found: C 70.50; H 3.39.

11-Hydoxy-_6H,7H_-7-(4-Hydroxy-3-coumarinyl)[1]benzopyrano[4,3-b][1]benzopyran-6-one (4c)

Pink powder, mp 235-237 °C; ^{1}H NMR (DMSO-D_6): δ 5.62 (s, 1H, CH), 6.57 (d, *J*=6.6 Hz, 1H, ArH), 6.71 (d, *J*= 6.7 Hz, 1H, ArH), 6.98 (d, *J= 7.0 Hz*, 1H, ArH), 7.31-7.73 (m, 7H, ArH), 8.08 (d, *J*=8.1 Hz, 1H, ArH), 9.79 (br s, OH-Ar), 12.12 (br s, OH-pyr) ; RMN ^{13}C (DMSO-D_6): δ 28.1 (C*), 102.7, 112.9, 113.8, 116.2, 116.4, 122.7, 123.9, 124.5, 129.1, 132.1, 132.4, 149.7, 151.9, 152.1, 157.3, 160.5. ms (ESI): m/z (% relative intensity): 449.2 (100%) ($M+Na^+$). Elemental analysis: Calcd. For $C_{25}H_{14}O_7$: C 70.42; H 3.31; Found: C 70.50; H 3.39.

9-Hydoxy-_6H,7H_-7-(4-Hydroxy-3-coumarinyl)[1]benzopyrano[4,3-b][1]benzopyran-6-one (4d)

Gray powder, mp 292-294 °C; ^{1}H NMR (DMSO-D_6): δ 5.67 (s, 1H, H*), 6.60 (s, , 1H, ArH) 6.68 (d, J= 6.70 Hz , 1H, ArH), 7.1 (d, J= 7.17Hz , 1H, ArH), 7.33-7.48 (m, 5H, ArH), 7.59 (t, 1H, ArH), 7.67 (t, 1H, ArH), 8.05 (d, *J*= 8.06 Hz, 1H, ArH), 9.39 (br s, OH-Ar), 12.24 (br s, OH-pyr.); RMN ^{13}C (DMSO-D_6): δ 28.7 (C*), 98.8, 113.9, 114.0, 115.2, 116.1, 116.4, 117.1, 122.6, 123.9, 124.5, 132.2, 132.4, 142.0, 142.1, 151.9, 152.2, 154.5, 160.5. ms (ESI): m/z (% relative intensity): 449.1 (100%) ($M+Na^+$). Elemental analysis: Calcd. For $C_{25}H_{14}O_7$: C 70.42; H 3.31; Found: C 70.50; H 3.39.

9-Nitro-_6H,7H_-7-(4-Hydroxy-3-coumarinyl)[1]benzopyrano[4,3-b][1]benzopyran-6-one(4e)

White powder, mp 312-315 °C; I.R υ (cm^{-1}): 3309, 3072, 1703, 1670, 1646, 1629, 1609, 1523, 1496, 1455, 1392, 1337, 1286, 1243, 1218, 1185, 1111, 1090, 1059, 904, 848, 754. ^{1}H NMR (DMSO-D_6): δ 6.20 (s, 1H, H*), 6.79 (d, *J*=8.8 Hz, 1H, ArH) 7.22–7.26 (m, 4H, ArH), 7.48–7.52 (m, 2H, ArH), 7.82 (d, *J*=7.2 Hz, 2H, ArH), 7.93 (dd, *J*=8.8 Hz, *J'*=2.8 Hz, 1H, ArH), 8.04 (d, *J*=8.0 Hz, 1H, ArH) ; RMN ^{13}C (DMSO-D_6): δ 28.6 (C*), 102.5, 112.5, 113.3, 116.1, 116.6, 117.6, 122.7, 123.1, 124.3, 124.4, 124.7, 125.0, 132.5, 132.9, 133.3, 138.3, 144.2, 152.0, 152.3, 154.3, 159.7, 160.1. ms (ESI): m/z (% relative intensity): 478.1 (100%) ($M+Na^+$). Elemental analysis: Calcd. for $C_{25}H_{13}O_8N$: C 65.94, H 2.88, N 3.08, Found: C 66.02, H 2.96, N 3.04.

9-Iodo-_6H,7H_-7-(4-Hydroxy-3-coumarinyl)[1]benzopyrano[4,3-b][1]benzopyran-6-one(4f)

White powder, mp 295-297 °C; ^{1}H NMR (DMSO-d_6, 300 MHz): δ 5.69 (s, 1H, CH), 7.16 (d, *J*=7.19 Hz, 1H, ArH), 7.31-7.48 (m, 5H, ArH), 7.57-7.71 (m, 3H, ArH), 8.05 (dd, *J*=8.07 Hz, *J'*=2.1 Hz, 2H, ArH), 8.07 (d, *J=8.09 Hz*, 1H, ArH), 12.33 (s, br, OH-pyr.); RMN ^{13}C (DMSO-D_6, 400MHz): δ 28.9, 102.80, 116.5, 116.6, 118.2, 118.9, 122.6, 124.5, 125.4, 126.3, 132.7, 132.8, 134.5, 137.4, 144.5, 152.4, 152.7, 152.8, 160.7. ms (ESI): m/z (% relative intensity): 558.9 (100%) $(M+Na)^+$. Elemental analysis: Calcd. for $C_{25}H_{13}IO6$: C 55.99, H 2.44, Found: C 56.02, H 2.56.

_6H,7H_-7-(4-Hydroxy-3-coumarinyl)[1]benzo[f]benzopyrano[4,3-b][1]benzopyran-6-one (4g)

Pink powder, mp 298-300 °C ; ^{1}H NMR (DMSO-D_6): δ 6.19 (s, 1H, CH), 7.26 (t, *J*=7.7 Hz, 2H, ArH) 7.42-7.63 (m, 7H, ArH), 7.69-7.74 (m, 1H, ArH), 7.93-7.99 (t, *J*=8.0 Hz, 2H, ArH), 8.16 (dd, 1H, *J*=8.2 Hz, *J'*= 2.1 Hz), 12.66 (br s, OH-pyr.); RMN ^{13}C (DMSO-D_6): δ 27.0 (C*), 101.3, 113.7, 115.8, 116.2, 116.5, 117.0, 122.7, 123.9, 124.5, 125.0, 127.2, 128.7, 129.2, 132.3, 132.6, 138.4, 152.0, 152.2, 160.5; ms (ESI): m/z (% relative intensity): 483.2 (100%) ($M+Na^+$). Elemental analysis: Calcd. For: $C_{29}H_{16}O_6$: C 75.65; H 3.50; Found: C 75.86; H 3.65.

3-(2-hydroxybenzoyl)-2H-chromen-2-one (5a)

Yellow powder, mp 175-177°C; I.R υ (cm^{-1}): 3403 (OH), 1716 (O=C-O); ^{1}H-NMR (DMSO-D_6): δ 6.90–6.97 (m, 2H, HAr), 7.40–7.50 (m, 3H, HAr), 7.67–7.74 (m, 2H, HAr), 7.86 (d, *J*=7.6 Hz, 1H, HAr), 8.34 (s, 1H, H-4), 10.69 (s, br, OH-11) ; ^{13}C NMR (DMSO-D_6) : δ 116.1, 116.9, 118.3, 119.2, 123.4, 124.8, 128.1, 128.8, 129.7, 130.8, 133.2, 135.2, 142.7, 153.7, 158.5, 191.8. Ms (ESI): m/z (% relative intensity): 267 $(M+H)^+$ (100). Elemental analysis: Calcd. for $C_{16}H_{10}O_4$: C 72.18 ; H 3.79 ; Found: C 72.02 ; H 3.60.

8-hydroxy-3-(2-hydroxybenzoyl)-2_H_-chromen-2-one (5b)

Yellow powder, mp 252-254 °C; ^{1}H-NMR (DMSO-D_6): δ 7.18 (d, *J=7.8 Hz,* 1H, HAr), 7.20 (t, 1H, HAr), 7.34 (d, *J*=7.6 Hz, 1H, HAr), 8.34 (s, 1H, H-4), 10.40 (s, 1H, OH-8), 10.77 (s,1H, OH-11); ^{13}C NMR (DMSO-D_6) : δ 116.9, 118.3, 119.2, 123.4, 124.9, 128.1, 120.8, 129.7, 130.8, 133.2, 135.2,

144.4, 146.5, 153.7, 158.5, 191.8. Ms (ESI): m/z (% relative intensity): 305 $(M+Na)^+$ (100). Elemental analysis: Calcd. for $C_{16}H_{10}O_5$: C 68.09 ; H 3.57 ; Found: C 68.12 ; H 3.60.

7-hydroxy-3-(2-hydroxybenzoyl)-2*H*-chromen-2-one (5c)

Yellow powder, mp 254-256 °C ; RMN ^{1}H (DMSO-D_6): δ 6.78 (s, 1H, HAr), 6.84 (d, *J=7.6 Hz,* 1H, HAr), 6.87 (d, *J*=8.0 Hz*,* 1H, HAr), 6.90 (t, 1H, HAr), 7.71 (d, *J*=7.8 Hz*,* 1H, HAr), 7.42 (t, 1H, HAr),7.59 (d, *J*=7.6 Hz*,* 1H, HAr), 8.28 (s, 1H, H-4), 9.93 (s, 1H, OH-7), 10.64 (s, 1H, OH-11); RMN ^{13}C (DMSO-D_6): δ 102.0, 110.9, 113.9, 116.8, 119.2, 123.5, 124.3, 130.9, 131.6, 134.7, 144.7, 156.4, 158.3, 158.5, 163.6, 192.5. Ms (ESI): m/z (% relative intensity): 305 $(M+Na)^+$ (100). Elemental analysis: Calcd. for $C_{16}H_{10}O_5$: C 68.09 ; H 3.57 Found: C 68.22 ; H 3.50.

3-(2-hydroxybenzoyl)-6-iodo-2*H*-chromen-2-one (5f)

Yellow powder, mp 252-234 °C; ^{1}H NMR (DMSO-D_6): δ 6.92-6.96 (m, 2H, ArH), 7.29 (d, *J*=7.3 Hz, 1H, HAr), 7.47-7.52 (m, 1H, ArH), 7.69 (d, *J*=7.7 Hz*,* 1H, HAr), 7.97 (d, *J*= 7.8 *Hz*, 1H, HAr), 8.26 (s, 1H, HAr), 8.27 (s, 1H, H-4), 10.74 (s, br, OH-11); ^{13}C-NMR (DMSO-D_6): δ 117.4, 117.5, 119.0, 119.9, 121.1, 123.8, 127.0, 130.2, 131.3, 136.0, 138.0, 141.7, 153.9, 158.1, 159.2, 192.0, 160.89. ms (ESI): m/z (% relative intensity): 414.9 (100) $(M+Na)^+$. Elemental analysis: Calcd. for $C_{16}H_9IO_4$: C 49.01 ; H 2.31 Found: C 48.92 ; H 2.40.

3-(2-hydroxybenzoyl)-2H-benzo[f]chromen-2-one *(5g)*

Yellow powder, mp 254-256°C; I.R (KBr): 3486 (OH), 1571 (C=C-aromatic); ^{1}H-NMR (DMSO-D_6): δ 6.93 (d, *J*=7.8 Hz*,* 2H, HAr), 7.49 (t, 2H, HAr), 7.72 (t, 2H, HAr), 7.65 (d, *J*=7.8 Hz*,* 1H, HAr), 8.10 (d, *J*=7.7 Hz*,* 1H, HAr), 8.30 (d, *J*=7.6 Hz*,* 1H, HAr), 8.63 (d, *J*=8.0 Hz*,* 1H, HAr), 9.13 (s, 1H, H-4), 10.78 (s, 1H, OH-11); ^{13}C-NMR (DMSO-D_6): δ 112.3, 116.2, 116.9, 119.0, 122.1, 123.3, 126.0, 127.1, 128.4, 128.6, 128.9, 129.7, 131.1, 134.4, 135.3, 138.7, 153.9, 157.6, 159.0, 192.8; ms (ESI): m/z (% relative intensity): 339.09 (100) $(M+Na)^+$. Elemental analysis: Calculated for: $C_{20}H_{12}O_4$: C 75.94; H 3.82; Found: C 75.80; H 3.75.

2.4. Evaluation of the free-radical scavenging properties of 4a-g and 5a-g

The DPPH radical scavenging capacity was measured from the bleaching of purple coloured ethanol solution of DPPH· according to the method described by L.L. Mensor et al, J.S. Lee et al [18, 19]. DPPH· stock solution was prepared by dissolving 4 mg DPPH· in 100 mL ethanol. Compounds **4** and **5** were dissolved in DMSO to obtain a solution of 10^{-1} M. Test compounds were diluted further with DMSO to get final concentrations of 0.05, 0.025 and 0.0125 mol/l for all the compounds, whereas the standard (ascorbic acid) was diluted to 0.1, 0.05, 0.025, 0.0125, 0.00625, 0.003125, 0.0015625 mol/l solutions respectively. Wells were loaded with 40 µL of tested sample and then with 2 mL of DPPH solution, all assays being carried out in triplicate. Negative control wells were loaded with 40 µL of DMSO and 2 mL of DPPH· solution. After vortexing, the mixtures were incubated at room temperature for 1 h in darkness at 25 °C, and then the absorbance of the plate was recorded at 517 nm. Ascorbic acid (AA) was used as standard for the antioxidant activity screening. A blank containing only ethanol with DMSO was used as the control. Each measurement was performed in triplicate.

2.5. Molecular docking studies

Molecular docking studies were conducted next to evaluate the potential of compounds **4a**,**5a** to inhibit p38 MAPK, an anticancer target enzyme. To this aim, **4a**,**5a** as well as the known inhibitor SB2, structurally belonging to the pyridinyl-imidazole family, were docked in the p38 MAPK active site, using iGEMDOCK v 2.1 program [20], to predict their binding mode, their interactions and their binding energies with this protein. Structures were drawn using MarvinSketch software [21] and the corresponding PDB files were imported in iGEMDOCK v2.1 software as ligands. The protein coordinates of p38 MAPK was downloaded from the Protein Data Bank [22] (PDB: 1a9u with resolution of 2.50 Å, corresponding to p38 MAPK protein complexed with inhibitor SB2). The active site was identified as a distance of 8 Å from the center of bound ligand SB2. All docking simulations were performed with standard docking, population size of 200, 70 generations and number of solutions of 2. Obtained binding modes and docking energies of **4a**,**5a** were compared with those of the potent inhibitor SB2.

2.6. Molecular dynamics studies

In order to evaluate the stability of docked complexes, **4a**-p38 MAPK, **5a**-p38 MAPK and **SB2**-p38 MAPK, we submitted them to 10 ns of molecular dynamics simulations, using the same protocol of molecular dynamics as in our previous work [23]. Thus, we used the Nano Molecular Dynamics software NAMD 2.12 [24] with CHARMM 36 force field. Ligands topologies were generated using the CHARMM General Force Field (CGenFF) web server. All complexes were solvated in a cubic water box of edge length 10 Å and then neutralized with NaCl. The particle mesh Ewald (PME) method [25] was used with a 12 Å nonbonded cutoff and a grid spacing of 1 Å to include the contribution of short/long-range interactions. Periodic boundary conditions (PBCs) [26] were used and temperature and pressure were maintained constant using Langevin thermostat (310 K) and Langevin barostat (1 atm), respectively. Then, the three systems underwent 5000 steps of steepest-descent energy minimization to remove atomic overlaps or improper geometries. After this, studied systems were equilibrated for 100 ps under the constant number of particles, pressure and temperature (NPT). Finally, the obtained systems were submitted to 10 ns of molecular dynamics using 2 fs time steps. Obtained results were visualized and analyzed using VMD software [27] and Discovery Studio visualizer [28].

3. Results and discussion

3.1. Chemistry

In our previous studies, we have shown that the condensation of 4-hydroxy-6-methyl-2*H*-pyran-2-one (TAL) **7** with salicylaldehyde derivatives **2a**, in a range of different solvents (reflux) and using different catalysts, afforded 3-acetoacetylcoumarins **8** in basic medium [29] and 10-(4-Hydroxy-6-methyl-2-oxo-2*H*-pyran-3-yl)-3-methyl-1*H*,10*H*-

pyrano[4,3-b]chromen-1-ones **9** in the presence of heteropolyacids (HPA) [30] (scheme 2). 4-hydroxycoumarin (or 4-hydroxybenzopyran-2-one) **1** might react in the same manner than its homologue **7**, via the strongly nucleophilic carbon at position C3. To investigate the reactivity of **1** in a Knoevenagel condensation with **2**, a first set of experiments was devoted to study the influence of the solvent and of a catalyst in the reaction outcome.

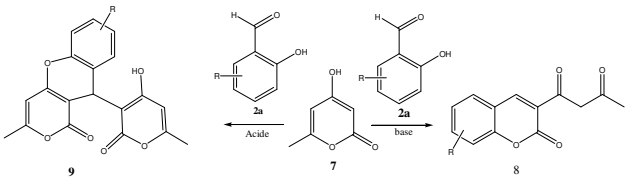

Scheme .2. Synthesis of 3-acetoacetylcoumarins **8** [29] and pyranyl-pyranpchromene **9**. [30]

a/- Solvent effect

We have started our work by revisiting the condensation of equimolar amounts of 4-hydroxycoumarin **1** and salicylaldehyde **2a** in refluxing ethanol, for 1.5 hours in the absence of any catalyst. This reaction led mainly to the formation of a yellowish solid after cooling and recristallisation from methanol, in moderate yield though (entry 1 of Table 1). MS (m/z 267 $[M+H]^+$) and ^1H NMR [10.69 ppm (br s, 1H, OH phenolic), 8.34 ppm (s, 1H, H-4), 6.90-7.82 ppm (9H, Har)] analyses were consistent with the formation of compound **5a**, a 1:1 adduct of **1** and **2a** (m/z 267 $[M+H]^+$) (Scheme 1). One can explain the formation of this compound by a Knoevenagel condensation of **1** with **2a** leading to compound **5a** after subsequent intramolecular translactonization (scheme 3).

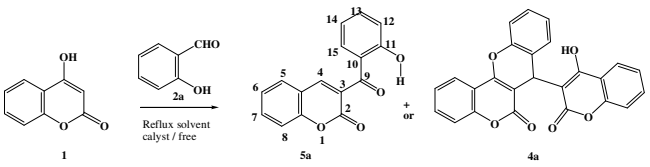

Scheme.3. Synthesis of 6*H*,7*H*-7-(4-Hydroxy-3-coumarinyl)[1]benzopyrano[4,3-b][1]benzopyran-6-one **4a** and 3-(2-hydroxybenzoyl)-2*H*-chromen-2-ones **5a**.

The reaction of salicylaldehyde **2a** with 4-hydroxycoumarin **1** was used as a model and was studied in different solvents (methanol, propanol, isopropanol, butan-2-ol, isobutanol, acetonitrile, THF and toluene) without any catalyst. Under these conditions, the reaction yielded a mixture of dicoumarol **4a** and translactonised product **5a**, which could be separated by simple recrystallisation in hot methanol. An optimized yield of 40 % was obtained in the presence of ethanol (Table 1, entry 1), protic solvents appearing as the most suitable for this transformation. In all these assays, translactonized compound **5a** was obtained as the major product, and was even formed in an exclusive manner in iPrOH or 2-butanol.

Table1 Synthesis of 6H,7H-7-(4-Hydroxy-3-coumarinyl)[1]benzopyrano[4,3-b][1]benzopyran-6-one **4a** and 3-(2-hydroxybenzoyl)-2*H*-chromen-2-ones **5a** under different reaction conditions.[a]

Entry	Solvent	Yields %	
		5a	**4a**
1	Ethanol	40	5
2	Methanol	33	21
3	Propanol	25	11
4	Isopropanol	26	-
5	Butan-2-ol	35	-
6	Isobutanol	34	11
7	ACN	7	2
8	THF	14	2
9	Toluene	No reaction	No reaction

[a] Reaction conditions: 4-hydroxycoumarin **1** (1 equiv), salicylaldehyde **2a** (1 equiv), refluxing solvent, 1.5 hours.
[b] Isolated yields.

b/- Influence of the catalyst

To investigate the influence of a catalyst in the reaction outcome, the same transformation was carried out under acid- (heteropolyacid, $H_3PMo_{12}O_{40}$) and base-catalyzed conditions (triethylamine) in refluxing ethanol/methanol. Under all these conditions, the reaction afforded two products **4a** and **5a** (Table 2) as well. However, acid catalysis mostly promotes the formation of dicoumarol **4a,** whereas NEt_3 affords exclusively the translactonization product **5a**. The formation of compound **4a** can be explained by a regioselective cascade reaction involving an acid/base catalyzed Knoevenagel condensation of **1** with **2a** leading to compound **3**, which undergoes a Michael addition in a specific position (**3a**) of another molecule of 4-hydroxycoumarin **1** affording intermediate **10**. A further cyclodehydration of **10** yielded the isolated 6*H*,7*H*-7-(4-Hydroxy-3-coumarinyl)[1]benzopyrano[4,3-b][1]benzopyran-6-one **4a**. Formation of **4a** is sensitive to nature of the solvent used and to the amount of HPA. The yield of **4a** increases with the increasing amount of $H_3PMo_{12}O_{40}$ (Table 2), best yield being obtained in the presence of 5 mol % catalyst in methanol.

When the reaction was performed using two equiv of **1** and one equiv of salicylaldehyde **2a** in the presence of 5 mol % of $H_3PMo_{12}O_{40}$ in methanol, **4a** was obtained in good yield (65%) (Table 2).

Table 2 Synthesis of **5a** and **4a** under different catalysts in ethanol and methanol.

Entry	Solvent	Catalyst (amount)	Yields (%)		Time (min)
			5a	**4a**	
1	Ethanol	$H_3PMo_{12}O_{40}$ (1%)	3	18	90
2		$H_3PMo_{12}O_{40}$ (2%)	4	22	90
3		$H_3PMo_{12}O_{40}$ (5%)	6	36	90
4		$H_3PMo_{12}O_{40}$ (8%)	traces	32	90
5		Triethylamine	53	-	20
6	Methanol	$H_3PMo_{12}O_{40}$ (1%)	5	38	90
7		$H_3PMo_{12}O_{40}$ (2%)	2	39	90
8		$H_3PMo_{12}O_{40}$ (5%)	traces	40	90
9		$H_3PMo_{12}O_{40}$ (8%)	traces	40	90
10		Triethylamine	78	-	20
11		$H_3PMo_{12}O_{40}$ (5%) [c]	-	65	90

[c] Reaction conditions: 4-hydroxycoumarin **1** (2 equiv), salicylaldehyde **2a** (1 equiv), refluxing methanol, $H_3PMo_{12}O_{40}$ (5%), 1.5 hours.

c/- Substituent effect

Subsequently, the reaction was applied to 2-hydroxyarylaldehydes **2b-f** and 2-hydroxynaphthaldehyde **2g**, which feature a range of electron-donating or electron-withdrawing substituents (Table 3). The reactions were carried out in MeOH or EtOH, without any catalyst or in the presence of $H_3PMo_{12}O_{40}$ (5 mol%). Alternatively, the molar ratio of both reagents **1** and **2a-g** was varied from 1:1 to 2:1 to study the impact of an excess of **1** on ratio or yield. The transformation proved efficient in all cases, yielding the expected benzoylchromenes **5b-g** and fused chromeno-chromens **4b-4g**. Better yields were obtained when using 2eq of 4-hydroxycoumarin **1** and 1eq of 2-hydroxyarylaldehydes **2b-f** and 2-hydroxy-naphthaldehyde **2g**. Unlike other salicyaldehyde derivatives, it was observed that 5-hydroxysalicylaldehyde **2d** leads to the formation of the same product **4d** in the presence or absence of the catalyst.

d/- Effect of time

An increase in reaction time (TLC monitoring), led to total selectivity (towards compounds **4**) with better yields than those observed when the reaction time was 90 minutes and the best yield was observed with 2-hydroxynaphthaldehyde **2g** (**4g**: 83%) (see Table 4).

Table 3 Synthesis of **5a-g** and/or **4a-g** in the absence of catalyst (in ethanol) and in the presence of $H_3PMo_{12}O_{40}$ (5 mol %) (in methanol), 4-hydroxycoumarin **1/** 2-hydroxyarylaldehydes **2b-f (**and 2-hydroxy-naphthaldehyde **2g)** (1:1 and 2:1 eq.), 1.5 hours.

Entry	Solvent	(amount of products)	Aldehyde	Conditions	Yields (%)	
					5a-g	**4a-g**
1	Ethanol	(1:1)	Salicylaldehyde **2a**	no catalyst	40	5
2			3-hydroxysalicylaldehyde **2b**		22	10
3			4-hydroxysalicylaldehyde **2c**		40	-
4			5-hydroxysalicylaldehyde **2d**		-	24
5			5-nitrosalicylaldehyde **2e**		No reaction	No reaction
6			5-Iodosalicylaldehyde **2f**		68	16
7			2-hydroxynaphtaldehyde **2g**		51	-
8	Methanol	(1:1)	Salicylaldehyde **2a**	$H_3PMo_{12}O_{40}$ (5 mol %)	6	36
9			3-hydroxysalicylaldehyde **2b**		-	32
10			4-hydroxysalicylaldehyde **2c**		-	40
11			5-hydroxysalicylaldehyde **2d**		-	43
12			5-nitrosalicylaldehyde **2e**		-	37
13			5-Iodosalicylaldehyde **2f**		10	41
14			2-hydroxynaphtaldehyde **2g**		-	48
15						
16		(2:1)	Salicylaldehyde **2a**	$H_3PMo_{12}O_{40}$ (5 mol %)	traces	65
17			3-hydroxysalicylaldehyde **2b**		-	53
18			4-hydroxysalicylaldehyde **2c**		-	64
19			5-hydroxysalicylaldehyde **2d**		-	60
20			5-nitrosalicylaldehyde **2e**		-	32
21			5-Iodosalicylaldehyde **2f**		traces	48
			2-hydroxynaphtaldehyde **2g**		-	65

Table 4. Synthesis of **4a-g** in the presence of $H_3PMo_{12}O_{40}$ (5 mol %), methanol and ratio of 4-hydroxycoumarin **1/ 2a-g** (2:1 eq).

Entry	Aldehydes	Compound	Time (h)	Yields (%)
1	Salicylaldehyde **2a**	**4a**	5	73
2	3-hydroxysalicylaldehyde **2b**	**4b**	4	62
3	4-hydroxysalicylaldehyde **2c**	**4c**	4	78
4	5-hydroxysalicylaldehyde **2d**	**4d**	3	76
5	5-nitrosalicylaldehyde **2e**	**4e**	6	40
6	5-Iodosalicylaldehyde **2f**	**4f**	4	63
7	2-hydroxynaphtaldehyde **2g**	**4g**	6	83

3.2. Mechanism of reaction

The first step of the proposal mechanism is a Knoevenagel condensation followed by dehydration, resulting in the formation of a stable chromone **3**, which might exist in two tautomeric forms **3a** and **3b**. In the last step, the chromone conjugate **3** undergoes two types of reactions according to the conformation of the intermediate: intramolecular translactonisation, which passes through the form **3b**, gives the compounds **5** and a Michael addition of a second molecule of 4 –hydroxycoumarin on the form **3a**, gives dicoumaroles **4**.

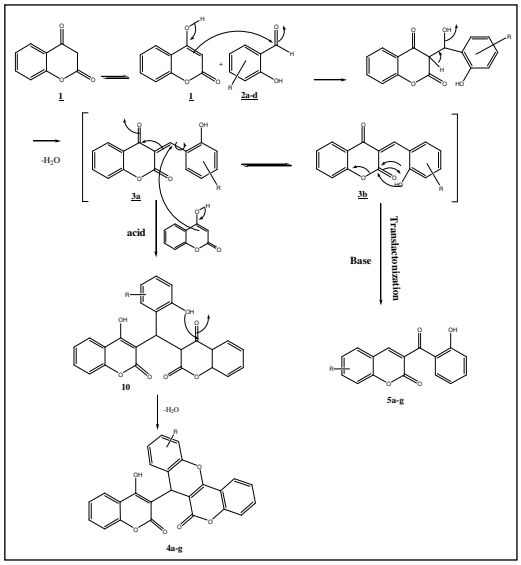

Scheme 3. Mechanism proposal for the synthesis of of 6*H*,7*H*-7-(4-Hydroxy-3-coumarinyl)[1]benzopyrano[4,3-b][1] benzopyran-6-one **4a** and 3-(2-hydroxybenzoyl)-2*H*-chromen-2-ones **5a**.

In order to explain the formation of the two products, we carried out the theoretical calculations of the formation enthalpies ΔH_f and the electrostatic potential of the charges (table 5) for the two rotamers **3a** and **3b** at B3LYP/6-31G* level of theory using ORCA software [31,32].

According to (Table 5), with almost all substrates (R=H, OH, NO_2, I) the endo-OH conformation **3b** is of lower energy than its exo-OH counterpart **3a**. This result might account for the increasing yield in product **5**, which results from intramolecular attack of proximal OH to coumarinyl carbonyl such as observed in structure **3a**.

On the other hand, if we look at the Mulliken charge values of the carbon atom of the C=O bond in position 2 of the coumarin nucleus, the latter is more positive in the **3b** form than in the **3a**, which favors the approach of the polar solvent and facilitates the translactonization unlike the apolar solvent.

Table 5 Calculated Gibbs energy of the two rotamers **3a** and **3b**.

R	Solvent	ΔH_f Kcal/mol x 10^{-3}	
		3a	**3b**
H	Ethanol	-575.45	-577.24
	Méthanol	-576,93	-579,05
	THF	-573,61	-571,14
3-OH	Ethanol	-622.78	-624.46
	Méthanol	-621,39	-619,00
	THF	-620,59	-618,07
4-OH	Ethanol	-620.19	-619.08
	Méthanol	-617,63	-622,61
	THF	-621,81	-616,99
5-OH	Ethanol	-620.99	-618.48
	Méthanol	-626,90	-629,16
	THF	-624,96	-624,79
5-NO_2	Ethanol	-703.53	-707,32
	Méthanol	-708,40	-708,22
	THF	-700,45	-706,41
5-I	Ethanol	578.63	-579.52
	Méthanol	-578,33	-579,52
	THF	-582,64	-577,72
Benzo[*f*]	Ethanol	-670.28	-670.51
	Méthanol	-669,76	-669,99
	THF	-670,23	-670,68

3.3. Antioxidant activity assessment

The antioxidant activity (free radical scavenging activity) of the synthesized **5** and **4** was evaluated using the 2,2-diphenyl-1-picrylhydrazyl free radical (DPPH·) scavenging assay [18, 19]. **Fig.1** shows the variation of absorbance versus concentration of the different compounds **4a-g, 5a-c, 5f-g** and of the standard ascorbic acid AA. Lower absorbance of the reaction mixture indicates higher free radical scavenging activity. The **IC_{50}** of the most active compounds are shown in **Fig.2** The capability to scavenge the DPPH· (or inhibition %) was calculated as follows:

$$\mathbf{RSA\ (\%) = [(Ac - As)/Ac] \times 100}$$

Where Ac is the absorbance of the control (absorbance of DPPH· ethanol solution without sample), and As is the absorbance of the tested compound after 60 min incubation.

These assays reveal that compound **5b** has excellent antioxidant activity (**IC_{50}= 0.2357 mg/ml**) followed by compound **4b** and **5f**. However, the other coumarinyl derivatives **5a, 5g**, **4e**, **4g** do not show any significant activity. According to the results obtained, we notice that the condensation of a second molecule of 4-hydroxycoumarin (compound **4b**, **4f**) leads to a decrease in antioxidant activity (SAR (%) **5b** > **4b**, **5f** > **4f**).

The results showed that the position of the hydroxyl groups has a significant impact on antioxidant activity. The best inhibition was observed when the OH group is in the meta position. Compared to the two compounds **5a** and **4a**, the introduction of an halogen substituent (Iodine) in the compounds **5f**, **4f** has led to an increase in activity.

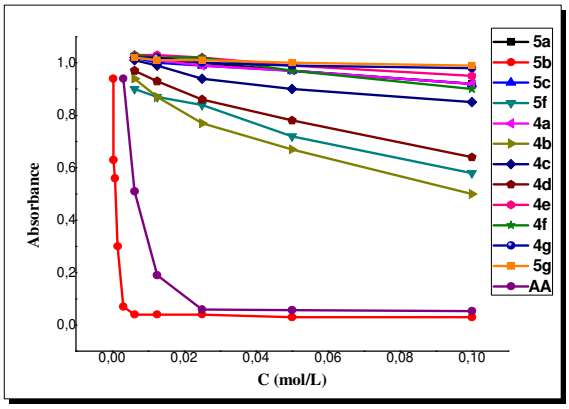

Fig.1. The variation of absorbance versus concentration of the different compounds **4, 5** and **AA**.

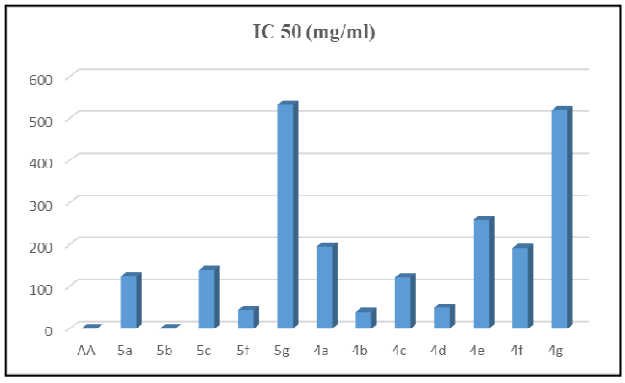

Fig.2. IC50 values of the antioxidant activity for compounds **5b**, **4b** and the standard **AA**.

3.4. Molecular docking

In order to evaluate the potential of our synthesized compounds against cancer pathology, we studied herein their binding mode, interaction and binding energies with p38 mitogen-activated protein kinase (p38 MAPK). The results show that almost all of the docked compounds bind at the same binding site in the active site of p38 MAPK as determined experimentally. Our docking method was first validated with the known ligand **SB2**, a potent inhibitor of p38 MAPK, by using the structure of protein-ligand complex PDB: 1a9u. Satisfyingly, comparison between the calculated and experimental positioning of SB2 into the protein shows that the docked conformation was close to the crystal one (as shown in Figure 3A). The RMSD between the two conformations was 0.75 Å, which is quite satisfactory as previously demonstrated [33].

Superposition of the docked conformations of synthesized compounds **4a** and **5a** on the X-ray structure of SB2 shows that binding modes of **4a** and **5a** are indeed most closely related to that observed in the crystallographic complex 1a9u, as shown in **(Fig. 3B)**.

Visualization of docked conformations of **4a** and **5a** shows that, the synthesized compounds are involved in hydrogen bonds and hydrophobic interactions with the residues of the protein active site. Compound **4a** interacted with different amino acids as shown in (**Fig. 3C**) and Table 6. It makes two hydrogen bonds with residue Asp168 and one with Lys53. On the other hand, compound **5a** makes one hydrogen bond with residue Ala51 and one with Lys53 (**Fig. 3C** and Table 6).

In table 6, we reported **4a** and **5a** binding energies, hydrogen bonds and interacting residues of the active site (< 4 Å). The binding energies between synthesized compounds and p38 MAPK protein are negative. It is worth noting that, the negative value of binding energy change reveals that the binding process is spontaneous and that the compound might be accepted as a drug.

On the other hand, the calculated binding energy of compound **4a** is lower than that of experimental ligand **SB2** (Table 6). Based on this result, it can be assumed that the synthesized compound **4a** shows higher affinities for p38 MAPK protein. In addition, interacting residues namely **Asp168**, **Leu104**, **Lys53** and **Ala51** are predicted by our docking model to be conserved in three studied compounds.

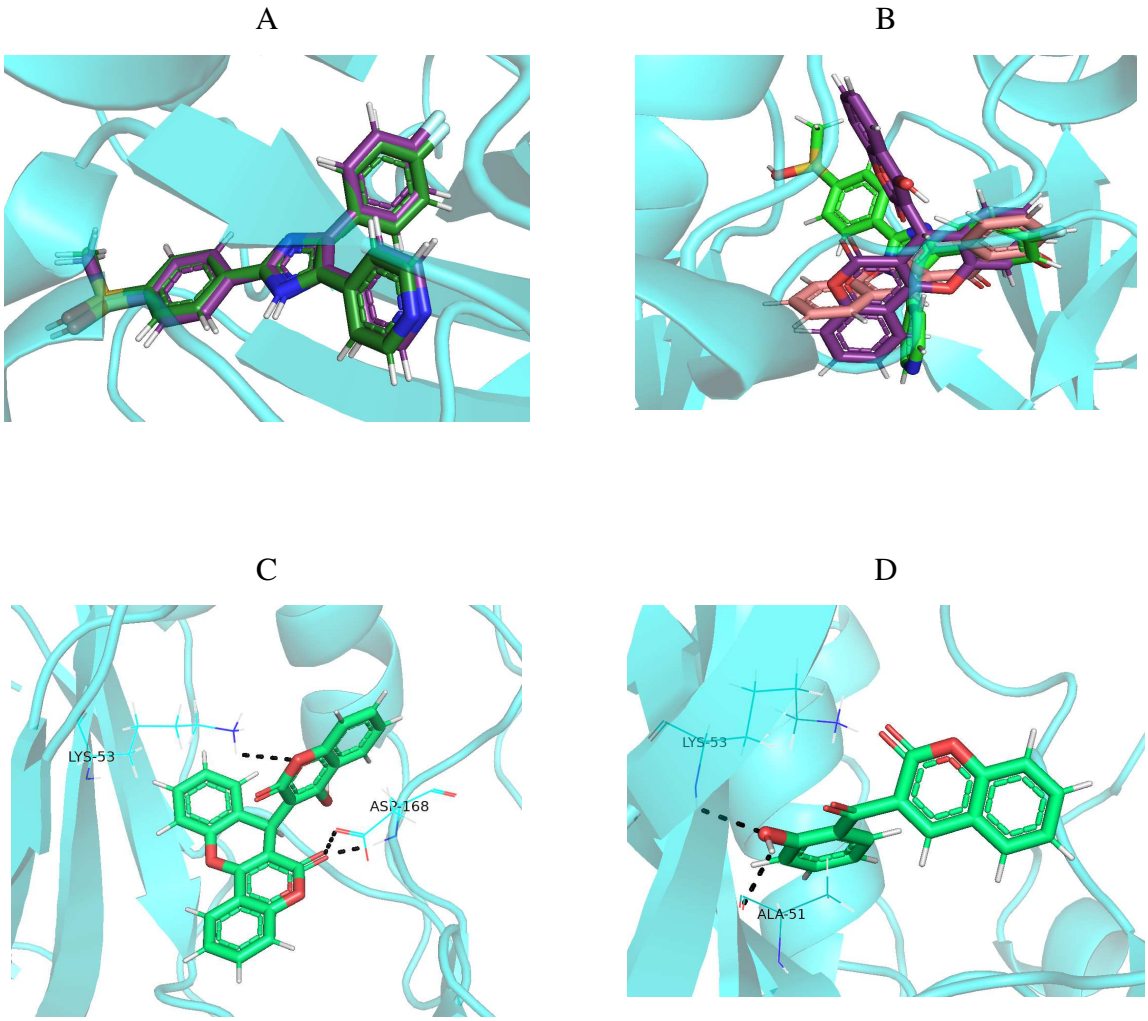

Fig. 3. Superimposition of A- docked (green) and experimental (magenta) structures of SB2; B- compounds **4a** (magenta), **5a** (pink) and experimental (green) structures of SB2); C and D- Hydrogen bond interactions between p38 MAPK active site residues and synthesized compounds C- **4a**, D- **5a**. The protein backbone was presented in blue ribbon.

Table 6 Interacting residues, hydrogen bonds, and binding energies of studied compounds as predicted by iGEMDOCK software.

Compound	Hydrogen bonds	Interacting residues	Binding energy
4a	Asp168 (2 Hbonds), Lys53	**Asp168**, Glu71, Leu167, **Leu104**, **Lys53**, **Ala51**, Met109,	-104.37
5a	Ala51, Lys53	**Asp168**, Leu167, **Leu104**, **Lys53**, Val38, **Ala51**	-77.13
SB2	Met109, Lys53	**Asp168**, Met109, His107, Thr106, Val105, **Ala51**, **Leu104**, **Lys53**, Val38, Tyr35	-98.80

3.5. Molecular dynamics studies

To confirm the binding mode and the stability of docked ligands **4a** and **5a** with p38 MAPK, molecular dynamics simulations were conducted. The stability of studied systems was evaluated based on change in RMSD of ligands in the protein active site and RMSD of carbons α of protein backbone and compared to those of experimental ligand SB2. Calculated RMSD plots of protein backbone Cα atoms of studied systems (**4a**-p38 MAPK, **5a**-p38 MAPK and **SB2**-p38 MAPK), through the 10 ns of molecular dynamics are reported in (**Fig. 4**).

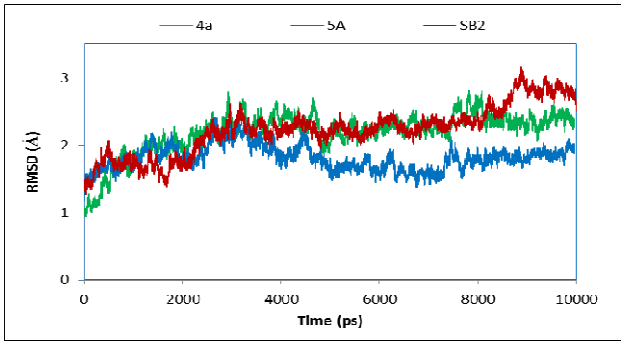

Fig. 4. RMSD plots of backbone Cα atoms of complexes 4a-p38 (green), **5a**-p38 (blue) and **SB2**-p38 (red).

This figure shows that the backbone Cα of **5a**-p38 and **4a**-p38 complexes show small fluctuations until 5 ns, where the complex reach stability at around 1.5 Å and 2.2 Å of RMSD, respectively, until the end of simulation. The RMSD of backbone Cα of **SB2**-p38 increases until 8.3 Å, after which it stabilizes at 2.8 Å until the end of simulation. Calculated RMSD plots of the three studied ligands **4a**, **5a** and **SB2**, through the 10 ns of molecular dynamics are reported in (**Fig. 5**).

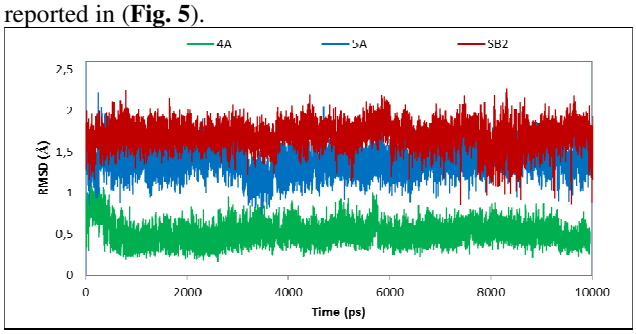

Fig. 5. RMSD plots of the studied compounds **4a** (green), **5a** (blue) and **SB2** (red) through the 10 ns of molecular dynamics simulations.

Analysis of results shows some differences between the three curves indicating some movements of studied compounds in the p38 active site. The calculated RMSD values of compound 4a decreases from 1 Å to 0.5 Å till 0.5 ns, and stays constant until the end of simulation time. This result confirms that the compound 4a reach equilibrium at 0.5 ns, revealing that it has converged during the simulation. On the other hand, the RMSD curve shape calculated for compound **5a** approaches a horizontal line during all the time of simulation, at the average value of RMSD of 1.4 Å, indicating that the compound reaches equilibrium and its change of conformation is very little. In contrary, the experimental compound **SB2** is stable until 7 ns, after which some fluctuations were observed.

The solvent accessible surface area (SASA) and the radius of gyration (rGyr) were calculated for the three studied complexes during the 10 ns of molecular dynamics simulation to illustrate the structural change of the protein and reported in (**Fig. 6**). These two parameters are widely used as the criterion of equilibrium [23,34].

A

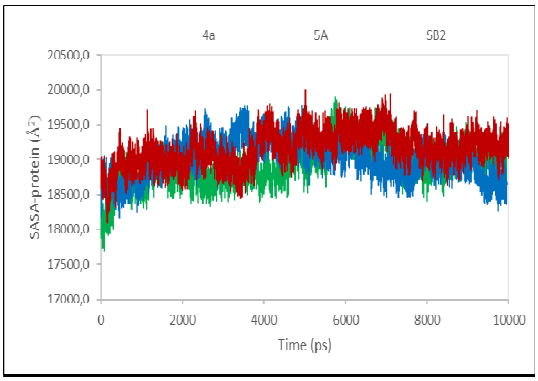

B

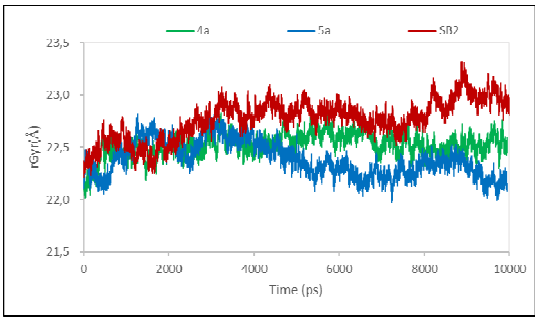

Fig. 6. Calculated Plots of A- protein SASA; B- radius of gyration for the three studied complexes **4a**-p38 (green), **5a**-p38 (blue and **SB2**-p-38 (red) through the 10 ns of molecular dynamics simulation.

The average values of total SASA calculated for SB2-p38 MAPK, **4a**-p38 MAPK, and **5a**-p38 MAPK complexes are 19178.6 Å^2, 18926.0 Å^2 and 19018.58 Å^2, respectively (**Fig. 6A**). The SASA of **4a**-p38 MAPK and **5a**-p38 MAPK complexes exhibit similar behavior as the experimental one up to 6 ns, following that a slight decrease in SASA of 5a-p38 MAPK complex was observed.

The calculated radius of gyration (rGyr) for **4a**-p38 MAPK, and **5a**-p38 MAPK complexes exhibits lesser fluctuations relative to the **SB2**-p38 MAPK revealing that the systems composed of our synthesized compounds **4a** and **5a**

and p38 MAPK protein arranged to a more compact conformation.

4. Conclusion

In this work, we have established a simple and efficient methodology to control the selectivity of the reaction of salicylaldehyde derivatives with 4-hydroxycoumarin in different conditions. It has been shown that, the synthesis of coumarin and bis-coumarin derivatives using 2-hydroxyarylaldehydes is highly dependent on the operating conditions used (nature of the solvent, absence/presence of the catalyst, the amount and the nature of the catalyst, nature of the substituent, reaction time). The absence of catalyst and the presence of a basic catalyst (triethylamine) favoured the formation of the compounds **5**. On the other hand, an acid catalyst ($H_3PMo_{12}O_{40}$, 5mol %) in the presence of 2 eq of 4-hydroxycoumarin **1**, using a protic polar solvent (methanol)**,** led to a total selectivity towards compounds **4**. The best yields were obtained for compounds **4** after increasing the reaction time.

From the antioxidant activity evaluation of the prepared compounds **4a-g** and **5a-g** one can highlight that derivative **5b** bearing a catechol group displayed the higher activity at low concentration. At higher concentration it became a pro-oxidant agent.

Molecular docking and molecular dynamics studies provided an insight into the molecular stability of synthesized compounds **4a** and **5a** in the p38 MAPK active site. Work is in progress to prepare a larger series of coumarinyl derivatives to enter SAR-studies aimed at evaluating their potential as anticancer agents.

Acknowledgments

Thanks are due to the Portuguese NMR Network. We thank Hilário Tavares (Department of Chemistry, University of Aveiro, 3810-193 Aveiro, Portugal) for performing the mass and NMR spectra.

Declaration of competing interest

The authors declare that they have no conflicts of interest.

References

[1] S. M. Sethna, N. M. Shah, The chemistry of coumarins, Chem. Rev. 36 (1) (1945) 1-62. https://doi.org/10.1021/cr60113a001.

[2] M.E. Riveiro, N. De Kimpe, A. Moglioni, R. Vazquez, F. Monczor, C. Shayo, C. Davio, Coumarins: Old Compounds with Novel Promising Therapeutic Perspectives, *Curr. Med. Chem.*17(2010)1325-1338. https://doi.org/10.2174/092986710790936284.

[3] M.E. Riveiro, D. Maes, R. Vazquez, M. Vermeulen, S. Mangelinckx, J. Jacobs, S. Debenedetti , C. Shayo, N. De Kimpe , C. Davio, *Bioorg. Med. Chem.* 17 (2009) 6547-6559. https://doi.org/10.1016/j.bmc.2009.08.002.

[4] R.O'Kennedy, R.D. Thornes, Coumarins: Biology, Applications, and Mode of Action, Chichester (UK): Wiley, (1997).

[5] D.L. Yu, M. Suzuki, L. Xie, S. L. Morris-Natschke, K. H. Lee, Recent progress in the development of coumarin derivatives as potent anti-HIV agents, *Med. Res. Rev.* 23 (2003) 322- 345. https://doi.org/10.1002/med.10034.

[6] Q.Y. Zhang, L.P. Qin, W.D. He, L. Van Puywelde, D. Maes, A. Adams, N. De Kimpe, Coumarins from *Cnidium monnieri* and their Antiosteoporotic Activity, *Planta. Medica.* 73(2007) 13-19. https://doi.org/10.1055/s-2006-951724.

[7] M. E. Riveiro, C. Shayo, F. Monczor, N. Fernandez, A. Baldi, N. De Kimpe, J. Rossi , S. Debenedetti, C. Davion, Induction of cell differentiation in human leukemia U-937 cells by 5-oxygenated-6,7-methylenedioxycoumarins from *Pterocaulon polystachyum, Cancer. Lett.* 210 (2004) 179-188. https://doi.org/10.1016/j.canlet.2004.03.015.

[8] R. D. H. Murray, J. Mendez, S.A. Brown,The Natural Coumarins: Occurrence, Chemistry, and Biochemistry. Chichester (UK): Wiley, (1982).

[9] V. T. Nguyen, S. Debenedetti, N. De Kimpe, Synthesis of coumarins by ring-closing metathesis using Grubbs' catalyst, *Tetrahedron. Lett.* 44 (2003), 4199-4201. https://doi.org/10.1016/S0040-4039(03)00902-X.

[10] D. Maes, S. Vervisch, S. Debenedetti, C. Davio. S. Mangelinckx, N. Giubellina, N. De Kimpe, Synthesis and structural revision of naturally occurring ayapin derivatives, *Tetrahedron*. 61 (2005) 2505-2511. https://doi.org/10.1016/j.tet.2004.12.061.

[11] R.Z. Batran, D.H. Dawood, S.A. El-Seginy , M. M. Ali , T. J. Maher, K. S. Gugnani, A. N. Rondon-Ortiz, New Coumarin Derivatives as Anti-Breast and Anti-Cervical Cancer Agents Targeting VEGFR-2 and p38α MAPK, *Arch. Pharm. Chem. Life. Sci*. 350 (9) (2017) 1-19. https://doi:10.1002/ardp.201700064.

[12] X. Jin, Q. Mo, Y. Zhang, Y. Gao, Y. Wu, J. Li, X. Hao, D. Ma, Q.Gao, P. Chen, The p38 MAPK inhibitor BIRB796 enhances the antitumor effects of VX680 in cervical cancer, *Cancer. Biol. Ther.* 17 (5) (2016) 566-576. https://doi:10.1080/15384047.2016.1177676.

[13] W.R. Sullivan, C.F. Huebner, M.A. Stahmann and K.P.Link, Studies on 4-Hydroxycoumarins. II. The Condensation of Aldehydes with 4-Hydroxycoumarins, *J. Am. Chem. Soc.* 65 (1943) 2288-2291. https://doi.org/10.1021/ja01252a008.

[14] M. Makhloufi-Chebli, M. Hamdi, A. M. Silva, S. F. Balegroune, Translactonisation intramoléculaire assistée par micro-ondes. Synthèse des coumarines, *J. Soc. Alger. Chim.* 18 (2008) 91-101.

[15] X. S. Wang, J. Zhou, K. Yang, M. M Zhang, Divergent Products Obtained from the Reactions of Salicylaldehyde and 4-Hydroxycoumarin in TEBAC-H_2O, KF-Al_2O_3-EtOH, and Ionic Liquid, *Synt. Comm.* 40 (2010) 3332-3345. https://doi.org/10.1080/00397910903419837.

[16] J. Riboulleau, C. Deschamps-Vallet, D. Molho, C. Mentzer, Benzopyrylium salts. I. Preparation and reductive heterocyclization of several 3-(o-hydroxybenzylidene)-2,4-dioxochromanes, *Bull. Soc. Chim. France,* 8-9 (1970) 3138-3144.

[17] P. de March, M. Moreno-Manas, J. L. Roca, The reactions of 4-hydroxy-2-pyrones with 2-hydroxybenzaldehydes. A note of warning, *J. of Het. Chem.*

21(5) (1984) 1371-1372. https://doi.org/10.1002/jhet.5570210525.

[18] A. Benazzouz, M. Makhloufi-Chebli, N. Khatir-Hamdi, B. Boutemeur-Khedis, A.M.S. Silva, M. Hamdi, A facile synthesis of new coumarin-3,4-dihydropyrimidin-2(1*H*)-ones/thiones dyads, *Tetrahedron*. 71 (2015) 3890-3894. https://doi.org/10.1016/j.tet.2015.04.028.

[19] L. Saher, M. Makhloufi-Chebli, L. Dermeche, S. Dermeche, B. Boutemeur-Khedis, C. Rabia, M. Hamdi, A. M.S. Silva, 10-(4-Hydroxy-6-methyl-2-oxo-2*H*-pyran-3-yl)-3-methyl-1H,10H pyrano[4,3-b]chromen-1-ones from a pseudo-multicomponent reaction and evaluation of their antioxidant activity, *Tetrahedron.* 74 (2018) 872-879. https://doi.org/10.1016/j.tet.2018.01.009.

[20] F. Neese, The ORCA program system, *Wiley interdiscip. WIREs. Comput. Mol. Sci*. 2(2012) 73–78. https://doi.org/10.1002/wcms.81.

[21] F. Neese, Calculation of the zero-field splitting tensor on the basis of hybrid density functional and Hartree-Fock theory, *J. Chem. Phys.* 127(16) (2007) 164112-164119. https://doi.org/10.1063/1.2772857.

[22] L.L. Mensor, F.S. Menezes, G.G. Leit~ao, A. S. Reis, C. T.dos Santos , S. C. Coube, S. G. Leitão, Screening of Brazilian plant extracts for antioxidant activity by the use of DPPH free radical method, *Phytother. Res.*15 (2001) 127-130. https://doi.org/10.1002/ptr.687.

[23] J.S. Lee, H.J. Kim, H. Park, Y.S. Lee, New Diarylheptanoids from the Stems of Carpinus cordata, *J. Nat. Prod.* 65 (2002) 1367-1370. https://doi.org/10.1021/np020048l.

[24] S. Bouaziz-Terrachet ,A. Toumi-Maouche , B. Maouche , S. Taïri-Kellou , Modeling the binding modes of stilbene analogs to cyclooxygenase-2: a molecular docking studyn, *J. Mol.Model.*16(12)(2010)1919–1929. https://doi.org/10.1007/s00894-010-0679-7.

[25] D. Roccatano, I. Daidone , M.A. Ceruso, C. Bossa , A.D. Nolan, Selective excitation of native fluctuation during thermal unfolding simulations: horse heart cytochrom c as a case study, *Biophys .J.* 84 (2003) 1876 – 1883. https://doi.org/10.1016/S0006-3495(03)74995-9.

[26] S. Hammad, S. Bouaziz-Terrachet, R. Meghnem, D. Meziane, Pharmacophore development, drug-likeness analysis, molecular docking, and molecular dynamics simulations for identification of new CK2 inhibitors, *J. Mol. Model.* 26 160 (2020). https://doi.org/10.1007/s00894-020-04408-2.

[27] H. Kai-Cheng, C. Yen-Fu, L. Shen-Rong, Y. Jinn-Moon, iGEMDOCK: a graphical environment of enhancing GEMDOCK using pharmacological interactions and post-screening analysis, *BMC Bioinf.* 12 (2011) 1-11. https://doi.org/10.1186/1471-2105-12-S1-S33.

[28] Marvin Sketch program, Chemaxon, http://www.chemaxon.com, (2009).

[29] http://www.rcsb.org/

[30] J.C. Phillips, R. Braun , W. Wang , J. Gumbart ,E. Tajkhorshid , E. Villa , C.Chipot , R.D. Skeel, L. Kalé , K. Schulten , Scalable molecular dynamics with NAMD, *J. Comput. Chem.* 26 (16) (2005) 1781–1802. https://doi.org/10.1002/jcc.20289.

[31] U. Essman , L. Perera , M.L. Berkowitz, T. Darden, H. Lee, L.G. Pedersen , A smooth particle mesh Ewald method, *J. Chem. Phys.* 103 (1995) 8577–8593. https://doi.org/10.1063/1.470117.

[32] W.L. Jorgensen, J. Chandrasekhar, J.D. Madura, R.W. Impey, M.L. Klein, Comparison of simple potential functions for simulating liquid water, *J. Chem. Phys.* 79 (1983) 926–935. https://doi.org/10.1063/1.445869.

[33] W. Humphrey, A. Dalke, K. Schulten, VMD: visual molecular dynamics, *J. Mol. Graph.*14 (1) (1996*)* 33–38 27–38. https://doi.org/10.1016/0263-7855(96)00018-5.

[34]http://www.accelrys.com.

Graphical Abstract

Selectivity control in the reaction between 2-hydroxyarylaldehydes and 4-hydroxycoumarin. Antioxidant activities and computational studies of the formed products

Leave this area blank for abstract info.

Kamilia Ould Lamara,[a] Malika Makhloufi-Chebli,[a] Amina Benazzouz-Touami,[a] Souhila Terrachet-Bouaziz,[b,c] Nejla Hamdi,[d, e] Artur M.S. Silva,[f] and Jean Bernard Behr [g]***

[a] *Laboratoire de Physique et Chimie des Matériaux LPCM, Faculté des Sciences, Université Mouloud Mammeri, 15000, Tizi Ouzou, Algeria.*

[b] *Department of Chemistry, Faculty of Sciences, University Mohamed Bouguerra, Boumerdes, Algeria.*

[c] *Laboratoire de Physico-Chimie Théorique et de Chimie Informatique, Faculté de Chimie, USTHB, BP 32 El Alia, 16111 Bab-Ezzouar, Alger, Algeria.*

[d] *Centre de Recherche Nucléaire de Draria (CRND), BP 43, Sebala, Draria, Algeria.*

[e] *Département du Génie de l'environnement, Ecole Nationale Polytechnique, 10 Avenue des Frères Ouadek, Hassen Badi, BP 182, 16200 El Harrach, Algiers, Algeria.*

[f] *QOPNA & LAQV-REQUIMTE, Department of Chemistry, University of Aveiro, 3810-193 Aveiro, Portugal.*

[g] *Université de Reims Champagne –Ardenne, Institut de Chimie Moléculaire de Reims (ICMR), CNRS UMR 7312, UFR Sciences Exactes et Naturelles, BP 1039, 51687 Reims Cedex 2, France.*

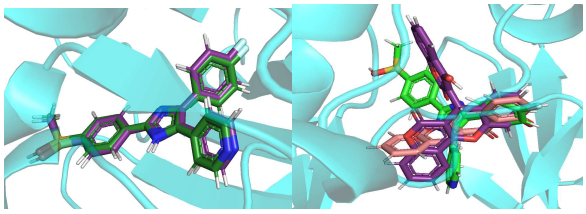

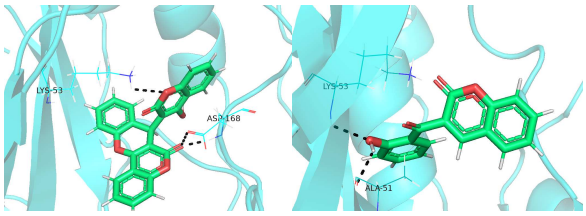

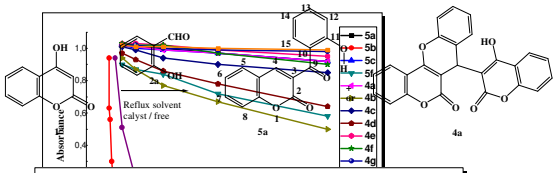

To create your abstract, type over the instructions in the template box below.

Fonts or abstract dimensions should not be changed or altered.